PCCP

Accepted Manuscript

This is an *Accepted Manuscript*, which has been through the Royal Society of Chemistry peer review process and has been accepted for publication.

Accepted Manuscripts are published online shortly after acceptance, before technical editing, formatting and proof reading. Using this free service, authors can make their results available to the community, in citable form, before we publish the edited article. We will replace this *Accepted Manuscript* with the edited and formatted *Advance Article* as soon as it is available.

You can find more information about *Accepted Manuscripts* in the Information for Authors.

Please note that technical editing may introduce minor changes to the text and/or graphics, which may alter content. The journal's standard Terms & Conditions and the Ethical guidelines still apply. In no event shall the Royal Society of Chemistry be held responsible for any errors or omissions in this *Accepted Manuscript* or any consequences arising from the use of any information it contains.

ROYAL SOCIETY OF CHEMISTRY

www.rsc.org/pccp

$KCaSrTa_5O_{15}$ Photocatalyst with Tungsten Bronze Structure for Water Splitting and CO_2 Reduction

Tomoaki Takayama,[1] Kentaro Tanabe,[1] Kenji Saito,[1†] Akihide Iwase,[1,2] Akihiko Kudo[1,2]*

[1]Department of Applied Chemistry, Faculty of Science, Tokyo University of Science, 1-3 Kagurazaka, Shinjuku-ku, Tokyo, 162-8601, Japan; [2]Photocatalysis International Research Center, Research Institute for Science and Technology, Tokyo University of Science, 2641 Yamazaki, Noda-shi, Chiba, 278-8510, Japan

**Corresponding author:Fax:+81-3-5261-4631, E-mail: a-kudo@rs.kagu.tus.ac.jp*

[†]Present address: Office for Development of Young Researchers, Research Planning and Promotion Division, Niigata University, 8050 Ikarashi 2-no-cho, Nishi-ku, Niigata 950-2181, JAPAN.

Abstract

$KCaSrTa_5O_{15}$ with tungsten bronze structure and 4.1 eV of a band gap showed activity for water splitting without cocatalysts. The activity was improved by loading NiO cocatalyst. The apparent quantum yield of optimized NiO-loaded $KCaSrTa_5O_{15}$ was 2.3% at 254 nm for water splitting. When CO_2 gas was bubbled into the reactant aqueous solution, Ag cocatalyst-loaded $KCaSrTa_5O_{15}$ produced CO and H_2 as reduction products of CO_2 and H_2O, respectively, and O_2 as an oxidation product of H_2O. The carbon source of CO was confirmed to be CO_2 molecules by using $^{13}CO_2$. The ratio of the number of electrons to that of holes calculated from the amounts of products (CO, H_2 and O_2) was almost unity. Additionally, the turnover number of electrons consumed for CO production to the total number of an Ag atom of the cocatalyst that was the active site for CO_2 reduction was 8.6 at 20 h. These results indicate that water was consumed as an electron donor for this photocatalytic CO_2 reduction in an aqueous medium. Thus, $KCaSrTa_5O_{15}$ with tungsten bronze structure has arisen as a new photocatalyst that is active for water splitting and CO_2 reduction utilizing water as an electron donor.

Introduction

An artificial photosynthesis system has been extensively studied to develop systems for CO_2 conversion to fuels and chemicals. Photocatalytic CO_2 reduction is one of the potential candidates for the artificial photosynthesis. Homogeneous and heterogeneous photocatalyst systems for CO_2 reduction have been studied. The homogeneous photocatalysts including Re-complex and Re-Ru-complex require sacrificial reducing reagents such as TEOA (Triethanolamine) to reduce CO_2 to CO and HCOOH.[1-6] Although a heterogeneous CdS photocatalyst shows activity for CO_2 reduction to form CO under visible light irradiation, sacrificial reagents are also indispensable.[7-8] Heterogeneous metal oxide photocatalysts which possess the ability for O_2 evolution by oxidation of water have been reported for the CO_2 reduction to form HCOOH, CO, CH_3OH and CH_4 in aqueous media without sacrificial reagents.[9-16] However, oxygen evolution in a stoichiometric amount is not observed in many cases. Among them, a ZrO_2 photocatalyst produces CO and H_2 as reduction products and O_2 as an oxidation product in a stoichiometric amount under UV irradiation.[14] Moreover, the activity and selectivity for CO_2 reduction to form CO are enhanced by loading a Cu cocatalyst on the ZrO_2 photocatalyst. $BaLa_4Ti_4O_{15}$[15] and Zn-doped Ga_2O_3[16] are highly active for CO_2 reduction using water as an electron donor when Ag cocatalyst is employed. Thus, metal oxide photocatalysts for water splitting can be applied to CO_2 reduction using water as an electron donor if suitable cocatalysts are chosen.

We have developed tantalum-based photocatalysts, such as $NaTaO_3$ and $NaTaO_3$:A (A = La and Sr) with perovskite structure, and $K_2LnTa_5O_{15}$ (Ln = La, Pr, Nd, Sm, Gd, Tb, Dy and Tm) with tungsten bronze structure, for highly efficient water splitting under UV irradiation.[17-19] The high activities for the tantalum-based photocatalysts are mainly due to their high conduction bands formed by Ta5d orbitals. We have also reported that a $BaLa_4Ti_4O_{15}$ photocatalyst[20] with two dimensional anisotropy of crystal structure for water splitting also shows activity for CO_2 reduction using water as an electron donor by loading highly dispersed Ag cocatalyst.[15] The selectivity for the CO_2 reduction is superior to that for water reduction to form H_2 even in an aqueous medium. On the other

hand, there is a tantalate group that possesses tungsten bronze structure with anisotropy to a c-axis of the crystal structure and the framework consisting of TaO_6 octahedra with corner sharing being similar to the perovskite structure as seen in $NaTaO_3$ of a highly efficient photocatalyst for water splitting. Therefore, the tantalates with tungsten bronze structure are expected to be active for water splitting and CO_2 reduction. In the present study, $KCaSrTa_5O_{15}$ with tungsten bronze structure[21] was prepared by a solid-state reaction, and their photocatalytic activities for water splitting and CO_2 reduction were investigated. The photocatalyst particles and cocatalysts were characterized using SEM, XPS and DRS.

Experimental

Preparation of $KCaSrTa_5O_{15}$

$KCaSrTa_5O_{15}$ was prepared by a solid-state reaction as follows. K_2CO_3 (Kanto Chemical: 99.0%), $CaCO_3$ (Kanto Chemical: 99.5%), $SrCO_3$ (Kanto Chemical: 99.9%) and Ta_2O_5 (Rare Metallic: 99.99%) were used as starting materials for the solid-state reaction. The carbonates and oxide were mixed in a molar ratio of K:Ca:Sr:Ta = 1.05:1:1:5 in an alumina mortar. The excess amount of potassium (5 mol%) was to compensate the volatilization.[22] The mixed powder was calcined in air at 1173 K for 1 h and subsequent 1423 K for 10 h in a platinum crucible. The excess potassium was washed out with water from the obtained powder.

Various cocatalysts were loaded by impregnation and photodeposition methods on the surface of $KCaSrTa_5O_{15}$ photocatalyst. NiO and Ag cocatalysts were loaded by an impregnation method. Photocatalyst powder was dispersed in aqueous solutions dissolving $Ni(NO_3)_2$ (Wako Pure Chemical: 98.5%) and $AgNO_3$ (Tanaka Rare Metal) in a porcelain crucible. The slurry solution was stirred with a glass rod during evaporation using a hot plate. Obtained powder was calcined in air at 575 K and 723 K for 1 h for loading the NiO and Ag cocatalysts, respectively. The NiO and Ag cocatalysts were reduced with H_2 at 773 K, if necessary. Ag, Ni, Ru, Rh, Pt, Cu and Au cocatalysts were photodeposited from aqueous solutions dissolving suitable amounts of $AgNO_3$, $Ni(NO_3)_2$, $RuCl_3$,

$RhCl_3$, H_2PtCl_6, $Cu(NO_3)_2$ and $HAuCl_4$ *in situ*.

$KCaSrTa_5O_{15}$ powders prepared by a solid-state reaction at several temperatures were examined by X-ray diffraction using Cu Kα radiation (Rigaku: Miniflex). Diffuse reflectance spectra of these powders were obtained using a UV-vis-NIR spectrometer (Jasco: UbestV-570) and were converted from reflection to absorption by the Kubelka-Munk method. Photocatalyst powders were observed by a scanning electron microscope (JEOL: JSM-6700F). Surface species of cocatalysts on photocatalysts were analyzed by X-ray photoelectron spectroscopy (Shimazdu: ESCA-3400; Mg anode). Metallic Ni (Nilaco: 99+%), NiO (Soekawa Chemical: 99.9%) and $Ni(OH)_2$ (Wako Pure Chemical: 95.0%) were employed as references for the XPS measurements. Binding energies were corrected using C 1s (285.0 eV) on a metallic Au foil (84.0 eV). [23]

Photocatalytic water splitting and CO_2 reduction

Photocatalytic reactions were conducted using an inner irradiation cell made of quartz with a 400 W high-pressure mercury lamp. 0.5 g of photocatalyst powder was dispersed in 350 mL of water. The Ar (99.99%) or CO_2 (99.995%) gas was continuously bubbled at 30 mL min^{-1} of a flow rate during the photocatalytic reaction. Gaseous products of H_2, O_2 and CO were determined with GC (Shimadzu: GC-8A with Molecular Sieve 5A, TCD and Ar carrier, and GC-8A with methanizer, Molecular Sieve 13X, FID and N_2 carrier). $^{13}CO_2$ (purity: 99.5 atom%) was also employed for an isotope experiment to confirm the carbon source for photocatalytic CO_2 reduction. ^{13}CO was analyzed by a GC-MS (Shimadzu: GC-MS Plus 2010, RESTEK: RT-Msieve 5A).

Results and Discussion

Characterization of $KCaSrTa_5O_{15}$

The X-ray diffraction patterns of the materials prepared at different calcination temperatures were assigned to $KCaSrTa_5O_{15}$ (PDF: 40-351) (Figure S1). Calcination below 1573 K gave small amounts of $Ca_2Ta_2O_7$ (PDF: 53-743) and an unknown compound as impurities (Figure S1 (a), (b) and

(c)), while the single phase of highly crystalline $KCaSrTa_5O_{15}$ was obtained by calcining at 1773 K for 10 h (Figure S1 (d)). The band gap of $KCaSrTa_5O_{15}$ was estimated to be 4.1 eV from the absorption edges except for the material prepared at 1173 K as shown in Figure 1. Primary particles of $KCaSrTa_5O_{15}$ with 200-300 nm of an average diameter aggregated, when they were prepared below 1573 K as shown in Figure 2 (a), (b) and (c). In contrast, the morphology of $KCaSrTa_5O_{15}$ prepared at 1773 K was rod as shown in Figure 2 (d), reflecting tungsten bronze structure in which TaO_6 octahedral units were connected with each other along the c-axis.

Effect of loading cocatalyst on water splitting and CO_2 reduction

Table 1 shows activity for water splitting over $KCaSrTa_5O_{15}$ under Ar gas flow. All samples prepared at different temperatures showed the activity for water splitting without cocatalyst. Moreover, the activities were drastically enhanced when NiO cocatalyst was loaded on $KCaSrTa_5O_{15}$. In contrast, the activities of $KCaSrTa_5O_{15}$ were not enhanced when Ni cocatalysts were loaded by a photodeposition, and an impregnation and H_2 reduction. NiO-loaded $KCaSrTa_5O_{15}$ prepared at 1423 K showed the highest activity. Although the initial activity of this photocatalyst was high, the rates of H_2 and O_2 evolution decreased at the initial stage as shown in Figure 3. H_2 and O_2 steadily evolved in a stoichiometric amount after the deactivation. The apparent quantum yield was 2.3% at 254 nm for water splitting (Figure S2). Thus, $KCaSrTa_5O_{15}$ with tungsten bronze structure has arisen as a new photocatalyst for water splitting.

The $KCaSrTa_5O_{15}$ photocatalyst was applied to CO_2 reduction as shown in Table 2. The pristine $KCaSrTa_5O_{15}$ produced only H_2 and O_2 without any reduction products of CO_2. This indicates that there were no active sites for CO_2 reduction on the surface of the $KCaSrTa_5O_{15}$ photocatalyst. Therefore, various cocatalysts were loaded to introduce active sites. Water splitting activity of $KCaSrTa_5O_{15}$ was enhanced when NiO and Au of effective cocatalysts[17, 24-25] for water splitting were loaded as observed for $BaLa_4Ti_4O_{15}$ photocatalyst.[15] No CO_2 reduction proceeded, when Ni, Ru, Rh, Pd, Pt and Au were loaded. When Cu cocatalyst was loaded, a small amount of CO evolved. In

contrast, Ag-loaded $KCaSrTa_5O_{15}$ photocatalyst produced CO from CO_2 as a reduction product regardless of loading methods of the Ag cocatalyst. In particular, the highest activity for CO_2 reduction was observed, when Ag cocatalyst was loaded by photodeposition and impregnation methods as shown in Table 2 and Figure S3. The fact that CO_2 was reduced on the Ag-loaded $KCaSrTa_5O_{15}$, but not on the pristine $KCaSrTa_5O_{15}$, indicates that Ag cocatalyst works as a reduction site of CO_2. Metallic Ag is a good electrocatalyst for reduction of CO_2 to CO.[26] The process of CO_2 reduction to CO on the Ag cocatalyst would be similar to that on the Ag electrocatalyst[27-28] as observed for $BaLa_4Ti_4O_{15}$[15] and Zn-doped Ga_2O_3[16] photocatalysts. A CO_2 molecule is reduced to CO_2^- adsorbed on Ag cocatalyst by a photoexcited electron. Although the redox potential of CO_2^- formation is -1.9 V,[27] the redox potential should become more positive due to stabilization by adsorption. The adsorbed CO_2^- is reacted with a H^+ ion in water to form an adsorbed –COOH. The adsorbed –COOH is subsequently reduced to become CO and OH^- by an another electron.[27-28]

H_2, O_2 and CO evolved steadily with a reaction time on the optimized Ag-loaded $KCaSrTa_5O_{15}$ photocatalyst as shown in Figure 4. The turnover number of electrons reacted for CO evolution to the number of the Ag atom in the cocatalyst calculated using the equation (1) was 8.6 at 20 h, and the ratio of electron to hole calculated using the equation (2) was unity. These results indicate that the CO_2 reduction over Ag-loaded $KCaSrTa_5O_{15}$ proceeded photocatalytically and water was consumed as an electron donor.

TON_{CO2} = (The number of electrons consumed for CO formation) / (The total number of a Ag atom in cocatalyst on $KCaSrTa_5O_{15}$) (1)

e^-/h^+ = (The number of electrons consumed for H_2 and CO formation) / (The numbers of holes consumed for O_2 formation) (2)

It has been reported that methane forms from not CO_2 but an organic contamination adsorbed on the photocatalyst surface.[29] Therefore, an isotope experiment using $^{13}CO_2$ was carried out to clarify the carbon source of CO formed. When the $^{13}CO_2$ gas was analyzed by a GC-MS using a MS-5A column, no peaks with mass numbers due to ^{12}CO and ^{13}CO were detected, indicating that

the $^{13}CO_2$ gas contained negligible amounts of ^{12}CO and ^{13}CO. In contrast, photocatalytic reduction of $^{13}CO_2$ over Ag-loaded $KCaSrTa_5O_{15}$ photocatalyst gave ^{13}CO and no ^{12}CO (Figure S4). Additionally, the ratio of electron to hole calculated from the products was about unity also in this isotopic experiment. Therefore, it was proven that CO was produced from CO_2 molecules over the Ag-loaded $KCaSrTa_5O_{15}$ photocatalyst.

Characterization of cocatalysts loaded on $KCaSrTa_5O_{15}$

NiO and Ag cocatalysts loaded on $KCaSrTa_5O_{15}$ before and after photocatalytic water splitting and CO_2 reduction were analyzed by scanning electron microscopy (SEM), X-ray photoelectron spectroscopy (XPS) and diffuse reflectance spectroscopy (DRS) in order to clarify the active states of these cocatalysts.

The particle size and morphology of NiO and Ni cocatalysts loaded on $KCaSrTa_5O_{15}$ photocatalysts were observed using SEM before and after photocatalytic water splitting (Figure S5). A particle size of NiO loaded by an impregnation method was about 10 nm (Figure S5 (a)). Small particle sizes of metallic Ni remained after H_2 reduction, though a part of metallic Ni sintered (Figure S5 (c)). The metallic Ni aggregated after the photocatalytic water splitting, and nano-particles of Ni were hardly observed (Figure S5 (d)). The shape of Ni loaded by a photodeposition method was not spherical particle being clearly different from that loaded by an impregnation method (Figure S5 (e)). Thus, the particle size and the shape of NiO and/or Ni cocatalysts after photocatalytic water splitting depended on the loading methods.

Figure 5 shows DRS of NiO and Ni-loaded $KCaSrTa_5O_{15}$ before and after photocatalytic water splitting. Non-loaded $KCaSrTa_5O_{15}$ was white and possessed 302 nm of an absorption edge (Figure 5 (a)). A color of $KCaSrTa_5O_{15}$ loaded with NiO by an impregnation method was gray and the background of the DRS arose at visible and near IR regions (Figure 5 (b)). A color of Ni/$KCaSrTa_5O_{15}$ obtained by an impregnation and subsequent H_2 reduction was pale brown and gave a broad absorption band with a peak around 400 nm (Figure 5 (d)). All Ni or NiO-loaded

photocatalysts were dark purple after photocatalytic water splitting giving broad absorption bands in visible light region (Figure 5 (c), (e) and (f)). This result suggests that the condition of nickel cocatalysts was similar to each other during photocatalytic water splitting regardless of the loading methods. The dark purple color did not quickly change after exposing to air.

Figure 6 shows XPS of Ni 2p of NiO and Ni cocatalysts loaded on $KCaSrTa_5O_{15}$ before and after photocatalytic water splitting. Binding energies of standard samples of metallic Ni, NiO and $Ni(OH)_2$ agreed with those of previous reports.[30] The surface of the standard NiO powder was covered with surface hydroxyl groups. NiO loaded on $KCaSrTa_5O_{15}$ by an impregnation method also gave peaks due to NiO and $Ni(OH)_2$ (Figure 6 (a)). Ni/$KCaSrTa_5O_{15}$ obtained by an impregnation and subsequent H_2 reduction gave XPS signals due to metallic Ni with NiO (Figure 6 (c)). All samples showed XPS signals mainly due to $Ni(OH)_2$ after photocatalytic water splitting (Figure 6 (b), (d) and (e)). $Ni(OH)_2$ is generally green, not dark purple as mentioned above. DRS of the samples after photocatalytic water splitting were different from that of $Ni(OH)_2$ (Figure S6). Therefore, the XPS signals due to $Ni(OH)_2$ observed for the samples after photocatalytic water splitting indicates the existence of not bulky $Ni(OH)_2$ but the surface nickel hydroxide as observed for a $NiO_x/SrTiO_3$ photocatalyst.[30] It has been reported that a color of a $NiO/InBO_4$ photocatalyst also changed to dark purple after photocatalytic water splitting.[31] Ultra fine NiO cocatalyst loaded on a $NaTaO_3$:La photocatalyst gives visible light absorption bands which are different from that of $Ni(OH)_2$.[32] Thus, active NiO cocatalyst loaded on the photocatalysts with wide band gaps has a unique character.

The impregnation method for loading the nickel cocatalyst was more effective than impregnation and subsequent H_2 reduction, and photodeposition methods for water splitting over the $KCaSrTa_5O_{15}$ photocatalyst as shown in Table 1. SEM and XPS measurements suggested that the most active $KCaSrTa_5O_{15}$ photocatalyst possessed the cocatalyst of fine NiO particles covered with surface nickel hydroxide.

SEM images of Ag loaded on $KCaSrTa_5O_{15}$ photocatalysts were also observed before and after photocatalytic CO_2 reduction (Figure S7). An impregnation method gave Ag cocatalyst with about 10

nm of the particle size before and after H_2 reduction (Figure S7 (a) and (c)). The Ag cocatalyst aggregated after photocatalytic CO_2 reduction (Figure S7 (b) and (d)). The growth of some Ag particles reached up to 50-100 nm. The particle size of Ag after photocatalytic CO_2 reduction was similar to that obtained by a photodeposition method (Figure S7 (e) and (f)).

Nano-sized metallic Ag particle generally gives a surface plasmonic absorption band in visible light region.[33] Therefore, DRS of samples before and after photocatalytic CO_2 reduction were measured as shown in Figure 7. Ag cocatalyst obtained by H_2 reduction was orange and gave a characteristic surface plasmonic absorption spectrum (Figure 7 (c)), while such a spectrum was not observed for Ag cocatalyst obtained by an impregnation method (Figure 7 (a)). All samples after photocatalytic CO_2 reduction gave similar absorption spectra to the sample obtained by H_2 reduction (Figure 7 (b), (d), (e) and (f)), although the intensities of the absorption spectra decreased after the photocatalytic reduction of CO_2. This result suggests dissolution and re-deposition of Ag during the photocatalytic reaction giving aggregated Ag particles as observed by SEM. Ag cocatalyst prepared by an impregnation method after the photocatalytic reduction of CO_2 also gave the similar absorption spectrum indicating that the Ag cocatalyst was reduced to fine metallic particles by photogenerated electrons. These results indicate that the metallic Ag giving the surface plasmonic absorption spectrum is an active site for the photocatalytic CO_2 reduction.

Conclusions

$KCaSrTa_5O_{15}$ (BG = 4.1 eV) with tungsten bronze structure has arisen as a new photocatalyst for water splitting and CO_2 reduction under UV light irradiation. $KCaSrTa_5O_{15}$ showed activity for water splitting without cocatalyst. In addition, NiO was an effective cocatalyst. The NiO cocatalyst activated during water splitting was dark purple and possessed a Ni hydroxide-shell/NiO-core structure as an active site for water reduction. The apparent quantum yield of optimized NiO-loaded $KCaSrTa_5O_{15}$ was 2.3% at 254 nm for the water splitting. On the other hand, Ag-loaded

$KCaSrTa_5O_{15}$ photocatalyst was active for CO_2 reduction to CO in an aqueous medium. The Ag cocatalyst activated during CO_2 reduction gave surface plasmonic absorption band in visible light region suggesting that fine metallic Ag particle is the active site for the CO_2 reduction. Isotope experiment using $^{13}CO_2$ revealed that the carbon source of produced CO was CO_2 molecules. Moreover, a stoichiometric amount of O_2 evolution and TON_{CO2} calculated from products was larger than 1 indicating that the CO_2 reduction to CO photocatalytically proceeded using water as an electron donor.

Acknowledgments

This work was supported by a Grant in Aid (No. 24246131) from the Ministry of Education, Sports, Science & Technology in Japan and the ENEOS hydrogen foundation.

References

(1) J. Hawecker, J. M. Lehn, R. Ziessel, *J. Chem. Soc., Chem. Commun.*, 1983, 536.

(2) J. Hawecker, J. M. Lehn, R. Ziessel, *Helv. Chim. Acta.*, 1986, **69**, 1990.

(3) H. Takeda, K. Koike, H. Inoue, O. Ishitani, *J. Am. Chem. Soc.*, 2008, **130**, 2023.

(4) H. Takeda, O. Ishitani, *Coord. Chem. Rev.*, 2010, **254**, 346.

(5) T. Yui, Y. Tamaki, K. Sekizawa, O. Ishitani, in *photocatalysis*, *Top. Curr. Chem.*, ed. C. A. Bignozzi, Springer, 2011, vol. 303, pp. 151-184.

(6) Y. Tamaki, K. Watanabe, K. Koike, H. Inoue, T. Morimoto, O. Ishitani, *Faraday Discuss.*, 2012, **155**, 115.

(7) S. M. Aliwi, K. F. Al-Jubori, *Sol. Energy Mater.*, 1989, **18**, 223.

(8) M. Kanemoto, K. Ishihara, Y. Wada, T. Sakata, H. Mori, S. Yanagida, *Chem. Lett.*, 1992, 835.

(9) K. Koči, L. Obalova, Z. Lacny, *Chem. Pap.*, 2008, **62**, 1.

(10) S. N. Habisreutinger, L. Schmidt-Mende, J. K. Stolarczyk, *Angew. Chem. Int. Ed.*, 2013, **52**,

7372.

(11) M. Tahir, N. S. Amin, *Energy Convers. Manage.*, 2013, **76**, 194.

(12) S. Navalon, A. Dhakshinamoorthy, M. Alvaro, H. Garcia, *ChemSusChem*, 2013, **6**, 562.

(13) J. Mao, K. Li, T. Peng, *Catal. Sci. Technol.*, 2013, **3**, 2481.

(14) K. Sayama, H. Arakawa, *J. Phys. Chem.*, 1993, **97**, 531.

(15) K. Iizuka, T. Wato, Y. Miseki, K. Saito, A. Kudo, *J. Am. Chem. Soc.*, 2011, **133**, 20863.

(16) K. Teramura, Z. Wang, S. Hosokawa, Y. Sakata, T. Tanaka, *Chem. Eur. J.*, 2014, **20**, 9906.

(17) A. Kudo, Y. Miseki, *Chem. Soc. Rev.*, 2009, **38**, 253.

(18) H. Kato, A. Kudo, *Catal. Today*, 2003, **78**, 561.

(19) A. Kudo, H. Okutomi, H. Kato, *Chem. Lett.*, 2000, 1212.

(20) Y. Miseki, H. Kato, A. Kudo, *Energy Environ. Sci.*, 2009, **2**, 306.

(21) D. Nelson, B. Scheetz, C. Abate, *The International Centre for Diffraction Data*, # 40-351.

(22) H. Kato, A. Kudo, *J. Phys. Chem. B*, 2001, **105**, 4285.

(23) M. P. Seah, *Surf. Interface Anal.*, 1989, **14**, 488.

(24) A. Iwase. H, Kato, A. Kudo, *Appl. Catal.B: Environmental*, 2013, **89**, 136.

(25) Y. Negishi, M. Mizuno, M. Hirayama, M. Omatoi, T. Takayama, A. Iwase, A. Kudo, *Nanoscale*, 2013, **5**, 7188.

(26) Y. Hori, K. Kikuchi, S. Suzuki, *Chem. Lett.*, 1985, 1695.

(27) Y. Hori, H. Wakebe, T. Tsukamoto, O. Koga, *Electrochim. Acta,* 1994, **39**, 1833.

(28) T. Hatsukade, K. P. Kuhl, E. R. Cave, D. N Abram, T. F. Jaramillo, *Phys. Chem. Chem. Phys.*, 2014, **16**, 13814.

(29) O. Ishitani, C. Inoue, Y. Suzuki, T. Ibusuki, *J. Photochem. Photobiol. A: Chem.*, 1993, **72**, 269.

(30) K. Domen, A. Kudo, T. Onishi, N. Kosugi, H. Kuroda, *J. Phys. Chem.*, 1986, **90**, 292.

(31) Q. Jia, Y. Miseki, K. Saito, H. Kobayashi, A. Kudo, *Bull. Chem. Soc. Jpn.*, 2010, **83**, 1275.

(32) H. Kato, K. Asakura, A. Kudo, *J. Am. Chem. Soc.*, 2003, **125**, 3082.

(33) K. Matsubara, T. Tatsuma, *Adv. Mater.*, 2007, **19**, 2802.

Table 1 Photocatalytic water splitting over $KCaSrTa_5O_{15}$ prepared at different temperatures.

Preparation Temperature / K	Cocatalyst	Loading method	Activity / μmol h^{-1}	
			H_2	O_2
1173	None	-	271	180
1173	NiO	Impregnation	639	263
1423	None	-	102	42
1423	NiO	Impregnation	1339	700
1423	Ni	Photodeposition	25	12
1423	Ni	Impregnation + H_2 red.	115	62
1573	None	-	106	47
1573	NiO	Impregnation	1270	644
1773	None	-	66	31
1773	NiO	Impregnation	212	95

Photocatalyst: 0.5 g, cocatalyst: 0.5 wt%, loading conditions: impregnation (573 K for 1 h in air), impregnation and subsequent H_2 reduction (773 K for 2 h in H_2 flow), photodeposition (*in situ*), reactant solution: water (350 mL), light source: a 400 W high-pressure mercury lamp, reactor: an inner irradiation cell made of quartz. $KCaSrTa_5O_{15}$ was prepared by a solid-state reaction at 1423 K for 10 h.

Table 2 Photocatalytic CO_2 reduction over various cocatalysts-loaded $KCaSrTa_5O_{15}$.

Cocatalyst	Loading Condition	Activity / μmol h^{-1}		
		H_2	O_2	CO
None	-	116	48	0
NiO	Impregnation[a]	764	398	0
Ni	Photodeposition	111	58	0
Cu	Photodeposition	216	100	trace
Ru	Photodeposition	28	13	0
Rh	Photodeposition	43	19	0
Ag	Photodeposition	53	37	8.1
Ag	Impregnation[b]	55	28	5.5
Ag	Impregnation[b]+H_2 red.	96	48	1.0
Pt	Photodeposition	62	23	0
Au	Photodeposition	584	269	0

Photocatalyst: 0.5 g, cocatalysts: 0.5 wt%, loading conditions: photodeposition (*in situ*), impregnation ([a] 573 K for 1 h in air, [b] 723 K for 1 h in air), impregnation and subsequent H_2 reduction (773 K for 2 h in H_2 flow), reactant solution: water (350 mL) dissolved with CO_2 under 1 atm, light source: a 400 W high-pressure mercury lamp, reactor: an inner irradiation cell made of quartz. $KCaSrTa_5O_{15}$ was prepared by a solid-state reaction at 1423 K for 10 h.

Figure captions

Figure 1 Diffuse reflectance spectra of $KCaSrTa_5O_{15}$ prepared at (a) 1173 K, (b) 1423 K, (c) 1573 K and (d) 1773 K for 10 h.

Figure 2 SEM images of $KCaSrTa_5O_{15}$ prepared at (a) 1173 K, (b) 1423 K, (c) 1573 K and (d) 1773 K for 10 h.

Figure 3 Water splitting over NiO(0.5 wt%)-loaded $KCaSrTa_5O_{15}$ photocatalyst. Photocatalyst: 0.5 g, reactant solution: water (350 mL) with Ar gas flow (30 mL min^{-1}), light source: a 400 W high-pressure mercury lamp, reactor: an inner irradiation cell made of quartz. $KCaSrTa_5O_{15}$ was prepared by a solid-state reaction at 1423 K for 10 h. NiO cocatalyst was loaded by an impregnation method.

Figure 4 CO_2 reduction over Ag(0.5 wt%)-loaded $KCaSrTa_5O_{15}$ photocatalyst in an aqueous medium. Photocatalyst: 0.5 g, reactant solution: water (350 mL) with CO_2 gas flow (30 mL min^{-1}), light source: a 400 W high-pressure mercury lamp, reactor: an inner irradiation cell made of quartz. $KCaSrTa_5O_{15}$ was prepared by a solid-state reaction at 1423 K for 10 h. The Ag cocatalyst was loaded by a photodeposition.

Figure 5 Diffuse reflectance spectra of (a) pristine $KCaSrTa_5O_{15}$ and (b)-(f) NiO(0.5 wt%) and Ni(0.5 wt%)-loaded $KCaSrTa_5O_{15}$ by various methods before and after water splitting. (b) Before and (c) after water splitting for the sample prepared by an impregnation method, (d) before and (e) after water splitting for the sample prepared by impregnation and subsequent H_2 reduction, (f) after water splitting for the sample prepared by a photodeposition. $KCaSrTa_5O_{15}$ was prepared by a solid-state reaction at 1423 K for 10 h.

Figure 6 X-ray photoelectron spectroscopy of Ni 2p of NiO(0.5 wt%) and Ni(0.5 wt%)-loaded $KCaSrTa_5O_{15}$. Nickel cocatalyst on $KCaSrTa_5O_{15}$ (a) before and (b) after water splitting for the sample prepared by an impregnation method, (c) before and (d) after water splitting for the sample prepared by an impregnation and subsequent H_2 reduction, (e) after water splitting for the sample prepared by a photodeposition. Standard sample of (f) $Ni(OH)_2$, (g) NiO, (h) metallic Ni foil. Reference data[30] are indicated as dashed lines respectively: Ni metal (853.1 eV), NiO (854.5 eV), $Ni(OH)_2$ (856.6 eV).

Figure 7 Diffuse reflectance spectra of Ag(0.5 wt%)-loaded $KCaSrTa_5O_{15}$ by various methods before and after CO_2 reduction. (a) Before and (b) after CO_2 reduction for the sample prepared by an impregnation method, (c) before and (d) after CO_2 reduction for the sample prepared by an impregnation and subsequent H_2 reduction, after CO_2 reduction for the sample prepared by a photodeposition at (e) 2h and (f) 20h, and (g) metallic and bulky Ag. $KCaSrTa_5O_{15}$ was prepared by a solid-state reaction at 1423 K for 10 h.

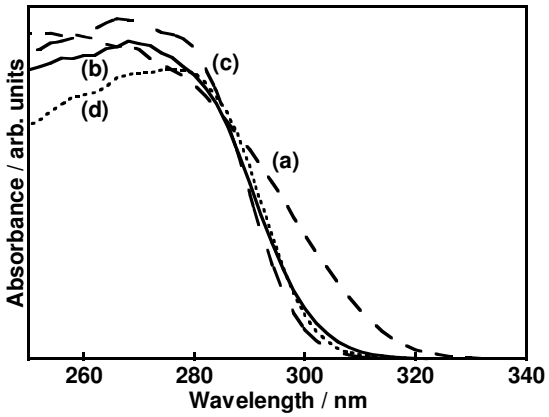

Figure 1 Diffuse reflectance spectra of $KCaSrTa_5O_{15}$ prepared at (a) 1173 K, (b) 1423 K, (c) 1573 K and (d) 1773 K for 10 h.

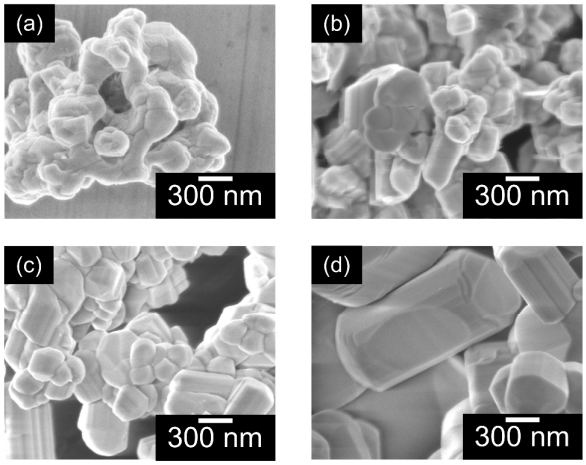

Figure 2 SEM images of $KCaSrTa_5O_{15}$ prepared at (a) 1173 K, (b) 1423 K, (c) 1573 K and (d) 1773 K for 10 h.

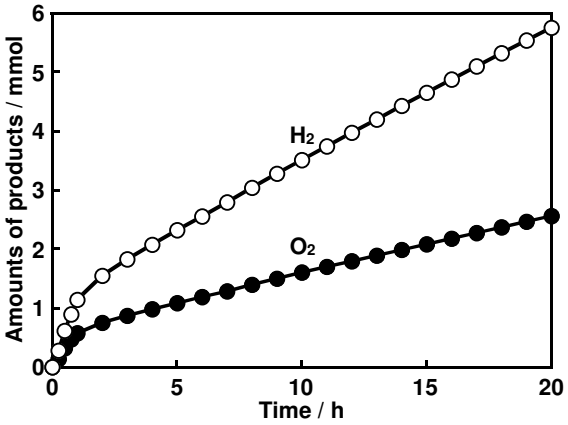

Figure 3 Water splitting over NiO(0.5 wt%)-loaded $KCaSrTa_5O_{15}$ photocatalyst. Photocatalyst: 0.5 g, reactant solution: water (350 mL) with Ar gas flow (30 mL min^{-1}), light source: a 400 W high-pressure mercury lamp, reactor: an inner irradiation cell made of quartz. $KCaSrTa_5O_{15}$ was prepared by a solid-state reaction at 1423 K for 10 h. NiO cocatalyst was loaded by an impregnation method.

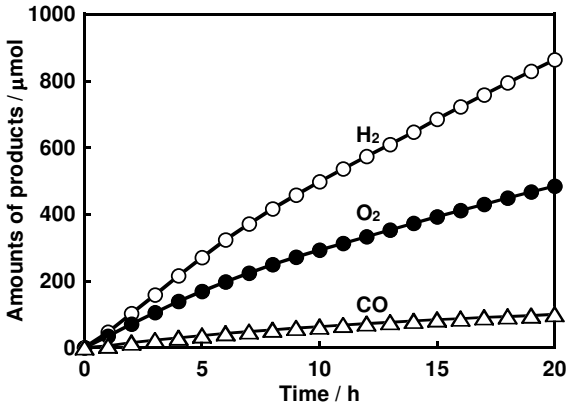

Figure 4 CO_2 reduction over Ag(0.5 wt%)-loaded $KCaSrTa_5O_{15}$ photocatalyst in an aqueous medium. Photocatalyst: 0.5 g, reactant solution: water (350 mL) with CO_2 gas flow (30 mL min^{-1}), light source: a 400 W high-pressure mercury lamp, reactor: an inner irradiation cell made of quartz. $KCaSrTa_5O_{15}$ was prepared by a solid-state reaction at 1423 K for 10 h. The Ag cocatalyst was loaded by a photodeposition.

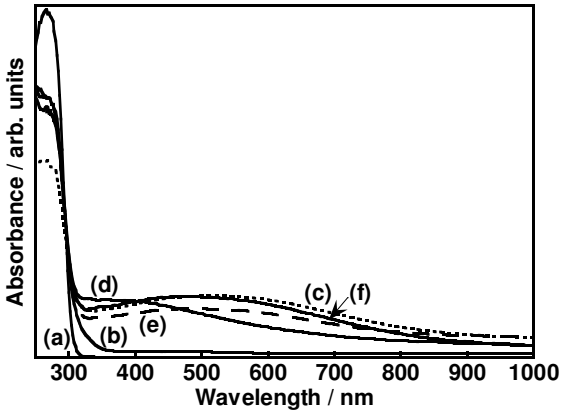

Figure 5 Diffuse reflectance spectra of (a) pristine $KCaSrTa_5O_{15}$ and (b)-(f) NiO(0.5 wt%) and Ni(0.5 wt%)-loaded $KCaSrTa_5O_{15}$ by various methods before and after water splitting. (b) Before and (c) after water splitting for the sample prepared by an impregnation method, (d) before and (e) after water splitting for the sample prepared by impregnation and subsequent H_2 reduction, (f) after water splitting for the sample prepared by a photodeposition. $KCaSrTa_5O_{15}$ was prepared by a solid-state reaction at 1423 K for 10 h.

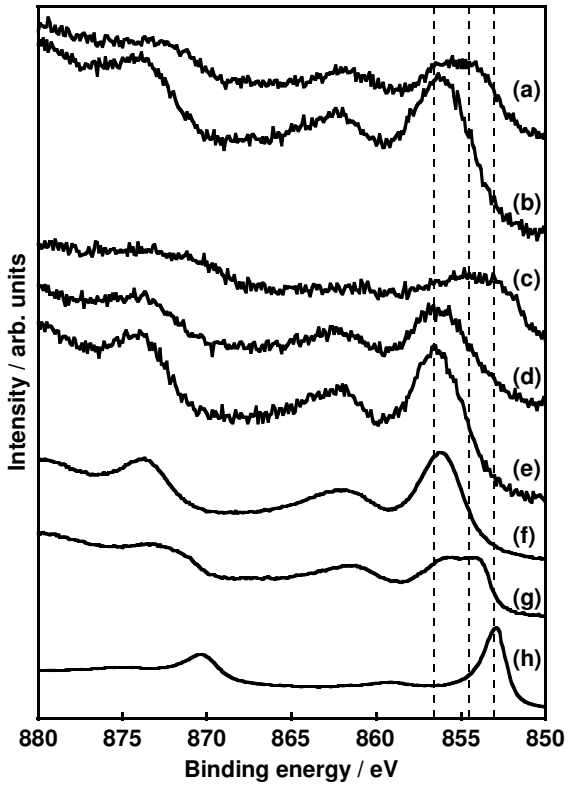

Figure 6 X-ray photoelectron spectroscopy of Ni 2p of NiO(0.5 wt%) and Ni(0.5 wt%)-loaded $KCaSrTa_5O_{15}$. Nickel cocatalyst on $KCaSrTa_5O_{15}$ (a) before and (b) after water splitting for the sample prepared by an impregnation method, (c) before and (d) after water splitting for the sample prepared by an impregnation and subsequent H_2 reduction, (e) after water splitting for the sample prepared by a photodeposition. Standard sample of (f) $Ni(OH)_2$, (g) NiO, (h) metallic Ni foil. Reference data[30] are indicated as dashed lines respectively: Ni metal (853.1 eV), NiO (854.5 eV), $Ni(OH)_2$ (856.6 eV).

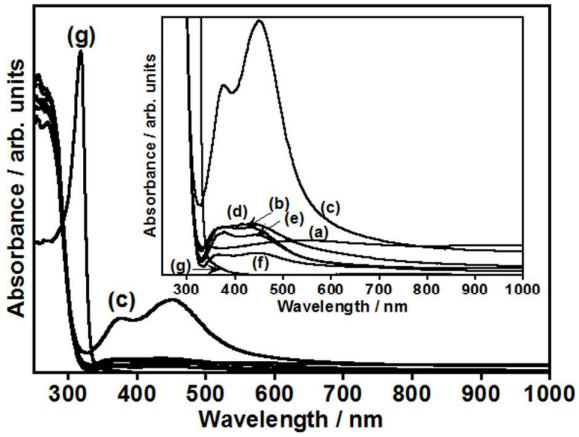

Figure 7 Diffuse reflectance spectra of Ag(0.5 wt%)-loaded $KCaSrTa_5O_{15}$ by various methods before and after CO_2 reduction. (a) Before and (b) after CO_2 reduction for the sample prepared by an impregnation method, (c) before and (d) after CO_2 reduction for the sample prepared by an impregnation and subsequent H_2 reduction, after CO_2 reduction for the sample prepared by a photodeposition at (e) 2h and (f) 20h, and (g) metallic and bulky Ag. $KCaSrTa_5O_{15}$ was prepared by a solid-state reaction at 1423 K for 10 h.